Supporting Information (SI) Appendix

for

"Cis and trans interactions between atlastin molecules during membrane fusion"

Tina Y. Liu[a], Xin Bian[b,1], Fabian B. Romano[a], Tom Shemesh[c], Tom A. Rapoport[a,2], and Junjie Hu[b,d]

[a] Howard Hughes Medical Institute and Department of Cell Biology, Harvard Medical School, 240 Longwood Avenue, Boston, MA 02115, USA.

[b]Tianjin Key Laboratory of Protein Sciences and Department of Genetics and Cell Biology, College of Life Sciences, Nankai University, Tianjin 300071, China

[c]Faculty of Biology, Technion–Israel Institute of Technology, Haifa 32000, Israel.

[d]National Laboratory of Macromolecules, Institute of Biophysics, Chinese Academy of Science, Beijing 100101, China

[1]Present address: Yale University, Boyer Center for Molecular Medicine, New Haven, CT 06519

[2]To whom correspondence should be addressed: tom_rapoport@hms.harvard.edu

Includes:

SI Materials and Methods

SI Figures, Fig. S1-S12

SI References

SI Materials and Methods

Constructs

For fusion, dynamic light scattering, and tethering assays, codon-optimized full-length *Drosophila melanogaster* atlastin (ATL) (residues 1-541) was cloned into pGEX-4T3 or pGEX-6P1, as described previously (1). Constructs encoding ATL-Sec61β and cyt-TM2 were cloned into pGEX-6P1, as described in (2). The cytosolic fragment of *Drosophila* ATL (cytATL; residues 1-422) with a C-terminal His_8 tag was cloned into pGEX-6P1.

For incorporation of azidophenylalanine into ATL, *Drosophila* cytATL was cloned into the pET28a vector and a mutant was generated in which the leucine codon at position 332 was replaced with an amber (TAG) codon using the QuikChange Site-Directed Mutagenesis Kit (Stratagene). For supported lipid bilayer experiments, a His_8 tag was added to the C-terminus of this mutant using the Gibson Assembly Master Mix (New England Biolabs). Wild-type cytATL was also cloned into the K27sumo vector to generate an untagged protein for competition experiments (see below). The K27sumo vector was a gift from Dirk Görlich (Max Planck Institute for Biophysical Chemistry, Göttingen, Germany) and can be used to express proteins fused to the C-terminus of the SUMO protein from *Saccharomyces cerevisiae*, Smt3p (3). All constructs were confirmed by DNA sequencing.

The pEVOL-pAzF vector, which encodes a *Methanocaldococcus jannaschii* aminoacyl-tRNA synthetase and suppressor tRNA pair, was a gift from Peter Schultz (Addgene plasmid # 31186)(4).

Expression and purification of ATL for fusion, dynamic light scattering, and tethering assays

ATL, ATL-Sec61β, and cyt-TM2 were expressed in *Escherichia coli* as GST fusions, as described (1, 2). The cells were lysed in A200 (25 mM HEPES (pH 7.5), 200 mM KCl, 1 mM EDTA, 2 mM β-mercaptoethanol (β-ME), and 10% (vol/vol) glycerol) supplemented with 1 mM phenylmethylsulfonyl fluoride (PMSF). The membranes were pelleted by centrifugation and solubilized in 2% or 4% (vol/vol) Triton X-100. The GST fusion

proteins were affinity-purified with glutathione Sepharose (GE Healthcare), and eluted with 10 mM reduced glutathione in A100 (25 mM HEPES (pH 7.5), 100 mM KCl, 1 mM EDTA, 2 mM β-ME, and 10% (vol/vol) glycerol) with 0.1% Triton X-100. Glutathione was removed using a PD-10 desalting column (GE Healthcare). The GST tag was cleaved off with thrombin or human rhinovirus 3C protease and removed using glutathione Sepharose. The cytosolic fragment of Drosophila ATL (residues 1-422) with a C-terminal His_8 tag (cytATL-His_8) was cloned and expressed in the same manner, except detergent was omitted and EDTA was removed with a PD-10 desalting column.

Expression, purification, and labeling of proteins for FRET and single-molecule tracking and photobleaching experiments

CytATL with an amber codon at position 332 was expressed as a C-terminally His_6-tagged protein in BL21(DE3) cells (cytATL-His_6). Azidophenylalanine was incorporated at position 332 by co-expressing cytATL-His_6 with the aminoacyl-tRNA synthetase and suppressor tRNA encoded in the pEVOL-pAzF vector (4). Expression was induced by the addition of 0.1 mM IPTG (Gold Biotechnology), 0.02% arabinose (Sigma), and 1 mM *p*-azidophenylalanine (Bachem), and continued for 16 h at 16^{o}C. Cells were harvested and lysed in HKG200 (25 mM HEPES (pH 7.5), 200 mM KCl, and 10% (vol/vol) glycerol) supplemented with 1 mM PMSF. The lysate was cleared by centrifugation for 1 h at 42,000 rpm and 4^{o}C in a Ti 45 rotor (Beckman), and cytATL-His_6 was isolated using Ni^{2+}-NTA resin (Thermo Scientific). The protein was then eluted with 200 mM imidazole in HKG100 (25 mM HEPES (pH 7.5), 100 mM KCl, and 10% (vol/vol) glycerol). CytATL-His_6 was labeled with a 20-fold molar excess of dibenzocyclooctyne (DBCO)-Cy5 or DBCO-Cy3 (Kerafast) for 16 h at 4^{o}C. Labeled proteins were treated with 10 mM dithiothreitol (DTT) to reduce disulfide bonds. Free dye, DTT, and imidazole were removed using a column packed with Sephadex G-50 superfine (GE Healthcare). The labeled proteins were then purified by gel filtration on a Superdex 200 column in HKG100 supplemented with 2 mM β-ME. The labeling efficiency was determined to be 55-60% by using the absorbance of Cy3 or Cy5 at 553 nm or 646 nm, respectively. These proteins were then used in solution FRET experiments. For supported lipid

bilayer experiments, His_8-tagged cytATL was expressed, purified, and labeled in the same manner. Alexa 647-labeled streptavidin was purchased from Invitrogen.

Expression and purification of untagged cytATL for supported lipid bilayer experiments

CytATL was expressed as a His_{14}-SUMO fusion protein from the K27sumo vector (3). Cells were lysed in HKG200 supplemented with 1 mM PMSF and 2 mM β-ME, and centrifuged for 1 h at 42,000 rpm and 4°C in a Ti 45 rotor. His_{14}-SUMO-cytATL was then isolated from the lysate using Ni^{2+}-NTA resin, and eluted with 250 mM imidazole. Imidazole was removed with a PD-10 column. The His-SUMO tag was cleaved off by the *Saccharomyces cerevisiae* SUMO protease, Ulp1p, and removed with Ni^{2+}-NTA resin. The protein was purified using gel filtration on a Superdex 200 column in HKG100 supplemented with 2 mM β-ME.

Liposome generation and ATL reconstitution

POPC (1-palmitoyl-2-oleyl-*sn*-glycero-3-phosphocholine), DOPS (1,2-dioleyl-*sn*-glycero-3-phospho-L-serine), dansyl-PE (1,2-dioleoyl-*sn*-glycero-3-phosphoethanolamine-N-(5-dimethylamino-1-naphthalenesulfonyl)), NBD-DPPE (1,2-dipalmitoyl-*sn*-glycero-3-phosphoethanolamine-N-(7-nitro-2-1,3-benzoxadiazol-4-yl)), rhodamine-DPPE (1,2-dipalmitoyl-*sn*-glycero-3-phosphoethanolamine-N-(lissamine rhodamine B sulfonyl)), DOGS-NTA-Ni^{2+} (1,2-dioleoyl-*sn*-glycero-3-[(N-(5-amino-1-carboxypentyl)iminodiacetic acid)succinyl] (nickel salt)), and biotinyl-DPPE (1,2-dipalmitoyl-*sn*-glycero-3-phosphoethanolamine-N-(cap biotinyl)) lipids were purchased from Avanti Polar Lipids. Texas Red- and Oregon Green-DPPE (1,2-dipalmitoyl-*sn*-glycero-3-phosphoethanolamine) were purchased from Invitrogen. Pre-formed liposomes of different compositions were prepared and reconstitution of ATL was performed as described (5).

Dynamic light scattering

ATL, ATL-Sec61β, or cyt-TM2 were reconstituted into pre-formed liposomes (83.5:15:1.5 mol % POPC:DOPS:dansyl-PE) (2, 5). CytATL-His_8 was immobilized on

liposomes with 5 mol % Ni^{2+}-NTA lipids (83.5:15:5:1.5 mol % POPC:DOPS:DOGS-NTA-Ni^{2+}:dansyl-PE) for 1 h at 4°C. The fluorescence of the dansyl dye (excitation at 336 nm and emission at 517 nm) in the liposomes was used to determine the total lipid concentration. Reactions (0.1 mM lipids, 60 μL) were performed in A100 supplemented with 5 mM $MgCl_2$. EDTA was omitted from the reaction buffer for experiments with cytATL-His_8. Reactions were equilibrated at 37°C and measurements were taken to ensure a stable baseline. Different nucleotides (1 mM) were then added. After 10 min, EDTA (18 mM) was added to inactivate ATL or imidazole (150 mM) was added to release cytATL-His from Ni^{2+}-NTA vesicles. Effective hydrodynamic radii of proteoliposomes were determined using a DynaPro Nanostar instrument (Wyatt), which detects light scattered at 90° to the incident beam. Laser power and attenuation levels were set automatically by the instrument. Measurements of particle radii were taken once every 30 sec or 1 min. The fold increase in vesicle radius was determined by dividing each measurement by the radius prior to nucleotide addition.

Tethering assay using light absorbance at 405 nm

Reaction conditions were the same as for dynamic light scattering. GTP, GTPγS, GMPPNP, or GDP were added at a 1 mM concentration to proteoliposomes (0.6 mM lipids, 30 μl) containing wild type ATL, ATL-Sec61β, cyt-TM2, or cytATL-His_8. For experiments with GDP/AlF_4^-, 1 mM GDP, 10 mM NaF, and 0.5 mM $AlCl_3$ were added sequentially to the reaction. After 40 min, 3 μL of 0.2 M EDTA-KOH, pH 7.5 was added to a final concentration of 18 mM EDTA to inactivate ATL, or imidazole was added to 150 mM to release cytATL-His from Ni^{2+}-NTA vesicles. Absorbance at 405 nm was measured at least once every minute in 384-well plates using a SpectraMax M5 Microplate Reader. In some figures, the absorbance was measured using a Biotek Synergy 4 plate reader, with a 100 μL reaction volume in a 96-well plate; in these experiments, EDTA was added to a concentration of 25 mM to stop the reaction after 40 min. The absorbance prior to nucleotide addition was set to zero.

Visual tethering assay

ATL or ATL-Sec61β was reconstituted into preformed liposomes with Texas Red-DPPE (84.5:15:0.5 mol % POPC:DOPS:Texas Red-DPPE) or Oregon Green-DPPE (84.5:15:0.5 mol % POPC:DOPS:Oregon Green-DPPE). The vesicles were mixed 1:1 (0.6 mM total lipids) in a reaction buffer of A100 supplemented with 5 mM $MgCl_2$. The mixture was warmed to 37°C, and different nucleotides were added. Samples of the reaction before and after nucleotide addition were diluted 1:50 into reaction buffer and a sample after nucleotide addition was diluted into A100 with 10 mM EDTA. The samples (6 μl) were spotted onto a glass coverslip (No. 1.5) and placed on a glass slide. Prior to use, glass coverslips were cleaned by sonication in 1 M NaOH for 20 min, followed by thorough rinsing with water, and sonication in 100% ethanol for 20 min. Vesicles stuck to the coverslip were visualized by confocal microscopy. The edges of the coverslip were sealed with VALAP (1:1:1 mixture of petrolatum, lanolin, and paraffin wax) to prevent dehydration of the sample during image collection. Oregon Green and Texas Red dyes were excited with 100mW 491 nm and 561 nm lasers and their emissions were collected with a quad pass dichroic mirror (Semrock, 405/488/568/647), and 525/50 nm and 620/60 nm filters (Chroma), respectively. Image collection was done using a Spectral Borealis-modified Yokogawa CSU-X1 spinning-disk confocal on a Nikon Ti motorized inverted microscope, with an 100x Plan Apo Lambda NA 1.45 objective lens, a Hamamatsu ORCA-AG cooled CCD camera, and MetaMorph 7 software. Image brightness and contrast were adjusted across the entire image, and merged images showing both dyes were generated using Fiji (6).

Liposome flotation assays

CytATL-His_8 vesicles, as generated for the tethering assay (1.5 mM lipids, 1:1,000 protein:lipid ratio), were mixed with Nycodenz in HKG100 at a 1:1 ratio (25 μl each) to reach a final concentration of 35% (wt/vol) Nycodenz. This mixture was placed in a thin-wall polypropylene tube (5 x 20 mm) and overlaid with 175 μL of 25% (wt/vol) Nycodenz in HKG100 and 25 μL of HKG100 lacking Nycodenz. After centrifugation in a TLS-55 rotor for 2.5 hours at 55,000 rpm and 4°C, five 50 μl fractions were collected from the top of the gradient. Top and bottom fractions were analyzed by SDS-PAGE. As

indicated in the figure legend, some samples of cytATL-His_8 vesicles were mixed with EDTA (18 mM) or imidazole (150 mM) before mixing with a Nycodenz solution, or cytATL-His_8 was mixed with vesicles lacking Ni^{2+}-NTA lipids.

For detecting association of full-length ATL with cytATL, proteoliposomes with ATL (1 mM lipids, 0.5 μM ATL; lipid composition was 83.5:15:1.5 mol % POPC:DOPS:dansyl-PE) were mixed with cytATL-His_6 (2 μM) in HKG100 supplemented with 2 mM β-ME and 5 mM $MgCl_2$. GTPγS (1 mM), GDP (1 mM), GDP/AlF_4^- (1 mM GDP, 10 mM NaF, 0.5 μM $AlCl_3$ added sequentially) or no nucleotide were added. The mixture was incubated for 20 min at room temperature and then subjected to flotation in a discontinuous Nycodenz gradient with 5 mM $MgCl_2$ present, as described above. Fractions were analyzed by SDS-PAGE analysis. After Coomassie Blue staining, the gel was scanned and image brightness and contrast were adjusted across the entire image using Adobe Photoshop CS5.1.

FRET experiments in solution

Cy3- and Cy5-labeled cytATL-His_6 were mixed 1:1 (0.5 μM each) in a reaction buffer of HKG100 supplemented with 2 mM β-ME and 5 mM $MgCl_2$ (200 μL total reaction volume). Cy3 was excited at 537 nm, and Cy3 and Cy5 fluorescence emissions were detected at 570 nm and 667 nm, respectively. Fluorescence was measured once every 30 sec in a black 96-well plate (Corning) using a SpectraMax M5 Microplate reader. The fluorescence was measured for 5 min, and nucleotide was added (GTP, GTPγS, GMPPNP, or GDP were added to 1 mM and GDP/AlF_4^- was generated by adding 1 mM GDP, 10 mM NaF, and 0.5 mM $AlCl_3$ sequentially). In competition experiments, unlabeled wild-type cytATL-His_6 (50 μM) or EDTA (18 μM) was added 20 min after addition of nucleotide. Relative FRET efficiencies were calculated as $I_A/(I_A + I_D)$, where I_A is the intensity of the acceptor (Cy5) fluorescence and I_D is the intensity of the donor (Cy3) fluorescence.

Lipid mixing assay

In vitro lipid mixing assays were performed as previously described (1, 2). Briefly, wild-type ATL, ATL-Sec61β, or cyt-TM2 were reconstituted into donor liposomes (82:15:1.5:1.5 POPC:DOPS:NBD-DPPE:rhodamine-DPPE) and acceptor liposomes (83.5:15:1.5 POPC:DOPS:dansyl-PE) at a protein:lipid ratio of 1:2,000 or 1:5,000, as indicated. The final lipid concentration in the lipid mixing reaction was 0.6 mM, unless otherwise indicated. Donor and acceptor vesicles were mixed at a 1:3 ratio in A100 supplemented with 5 mM $MgCl_2$. GTP was added to 1 mM to start the fusion reaction, and the fluorescence intensity of NBD was monitored with an excitation of 460 nm and emission of 538 nm using a SpectraMax M5 Microplate Reader or Biotek Synergy 4 plate reader. The maximal NBD fluorescence was determined after addition of dodecyl maltoside. The initial NBD fluorescence prior to nucleotide addition was set to zero, and the change in fluorescence was divided by the maximal fluorescence to obtain the % change in NBD fluorescence. Background fluorescence values in the absence of nucleotide were subtracted from the curves.

GTPase assays

The GTPase activities of ATL and cytATL proteins were determined using the EnzChek phosphate (P_i) assay kit (Invitrogen). For testing cytATL, 100 μl reactions containing 1 μM cytATL-His_6, 200 μM 2-amino-6-mercapto-7-methylpurine riboside (MESG), and 0.1 units purine nucleoside phosphorylase (PNP) in HKG100 supplemented with 2 mM β-ME were mixed in the presence of 0.5 mM GTP and warmed to 37°C. Reactions were initiated by addition of 5 mM $MgCl_2$. The absorbance at 360 nm was measured for at least 15 min in a 96-well plate using a SpectraMax M5 Microplate reader, with measurements taken every 30 sec. Control reactions without $MgCl_2$ were run in parallel, and were subtracted from the curves.

For testing full-length ATL, reactions of 100 μL contained 20 mM Tris-HCl (pH 7.5), 1 mM $MgCl_2$, 200 μM MESG, 0.1 units PNP, and 0.5 μM wild type or mutant ATL reconstituted into liposomes at a protein:lipid ratio of 1:2,000. Reactions were incubated for 30 min at 37°C, and initiated by the addition of 0.5 mM GTP. The absorbance at 360

nm was measured in a 96-well plate every minute over 60 min at 37°C using a BioTek Synergy 4 plate reader. Rates of P_i release were calculated based on a standard curve.

Supported lipid bilayer formation

The reaction chamber for supported-bilayer experiments was assembled by fixing a plastic ring (6 mm diameter) onto a plasma-cleaned No. 1.5 glass coverslip. For bilayer formation, small unilamellar vesicles (SUVs) were prepared by sonication of a 3 mM lipid solution (75:15:10 mol % POPC:DOPS:DOGS-NTA-Ni^{2+} for experiments with cytATL-His or 84:15:1 mol % POPC:DOPS:biotinyl-DPPE for experiments with streptavidin) in HK (25mM HEPES (pH 7.5), 100 mM KCl). Reaction chambers were incubated for 30 min at 23^{o}C with 50 µl of the SUV suspension supplemented with 1 mM $CaCl_2$ to favor bilayer formation. Subsequently, chambers were supplemented with 2 mg/ml bovine serum albumin (BSA) for passivation, incubated for 10 min at 23^{o}C, rinsed six times with HKG100 containing 2 mM β-ME, and then supplemented with 2 mg/ml BSA for passivation.

TIRF Microscopy

Image acquisition took place in HKG100 supplemented with 2 mM β-ME at 23^{o}C. All images were collected using a Nikon Ti-E motorized inverted microscope equipped with 100x Plan Apo 1.45NA TIRF objective lens, the Perfect Focus System for continuous maintenance of focus, a Nikon motorized TIRF illuminator, and Prior Proscan II linear-encoded motorized stage, filter wheels and shutters. Cy3 and Cy5 dyes were excited using the 561nm and 647nm laser lines of an Agilent MLC400B monolithic laser combiner. For FRET experiments, Cy3 and Cy5 emissions were collected through a Dual-View simultaneous two-channel imaging device (bandpass emission filters 510/30 and 650/75) into a Hamamatsu C9100-13 EM-CCD camera. For single-molecule tracking and photobleaching experiments, Cy5 fluorescence was collected using an Andor DU-897 EM-CCD camera (73 nm pixel size with the same setup as described above). The instrument was controlled with the Nikon NIS Elements image acquisition software. For time-lapse single-molecule tracking experiments, images were collected at a rate of 20 frames per second with constant illumination and 2x2 camera binning.

For FRET experiments, images were collected using no camera binning and a 50 ms exposure time.

FRET measurements and single-molecule tracking on supported lipid bilayers

His_8-tagged cytATL was added above a freshly formed supported lipid bilayer at the concentrations indicated in figure legends (total reaction volume of 70 µl). Chambers were incubated for 30 min at 23°C to allow membrane binding, rinsed five times with HKG100 containing 2 mM β-ME and then supplemented with 2 mg/ml BSA for passivation. To assay the effect of nucleotide analogs on cytATL dimerization, the chamber was supplemented with 5 mM $MgCl_2$ and different nucleotides were added. GTP, GTPγS, GMPPNP and GDP were added to a concentration of 1 mM, and GDP/AlF_4^- was generated by adding 1 mM GDP, 10 mM NaF, and 0.5 mM $AlCl_3$ sequentially to the chamber. Images were collected 10 min after addition of GTP or 30 min after addition of GDP/AlF_4^-, GTPγS, GMPPNP or GDP. For competition experiments, untagged wild-type cytATL was then added and the chamber was incubated for 10 min at 23°C before imaging. Mean fluorescence values were quantified using ImageJ, and relative FRET efficiencies were calculated as $I_A/(I_A + I_D)$, where I_A is the intensity of the acceptor (Cy5) fluorescence and I_D is the intensity of the donor (Cy3) fluorescence. The acceptor fluorescence was corrected for bleed-through of donor emission and direct excitation of the acceptor. Both donor and acceptor fluorescence were corrected for background.

Single molecules undergoing two-dimensional diffusion on supported lipid bilayers were tracked using U-Track software (7). Diffraction-limited light sources were automatically detected on each frame of time-lapse movies using Gaussian fits (8). Individual random-walk tracks were constructed using a maximum gap closing of three frames and a Brownian search radius of one to seven pixels (7). Plots of time-lapse fluorescence for single particles were generated using the amplitude output of Gaussian fits, and these were manually analyzed to quantify the number of bleaching steps per track. The 2D diffusion coefficient of single particles was calculated within the U-track software (7) using moment-scaling spectrum analysis (9, 10).

Modeling of ATL-mediated vesicle tethering

Formation of trans dimers between proximal vesicles

We assume that the formation of trans dimers between vesicles with radii of $R = 80nm$ becomes possible when two vesicles come within a minimal distance, $\delta = 2L_{ATL}$, where $L_{ATL} \approx 10nm$ is the length of an ATL monomer in crystal form 2 (1, 11). While cis dimers may form anywhere on the surface of the vesicles, trans dimer formation is restricted to a cap-shaped region on each vesicle, in which the distance between the two vesicle surfaces is δ or less. Since ATL molecules diffuse rapidly on a membrane (D=1.3 $\mu m^2/s$; Fig. S10C), the rate of trans dimer formation is related to the rate of cis dimer formation by

$$k_{on}^{(trans)} \simeq k_{on}^{(cis)} \chi \qquad \textbf{(1)}$$

, where χ is the ratio between the surface area of the cap region to the surface area of the entire vesicle:

$$\chi = \frac{\delta}{4R} \qquad \textbf{(2)}$$

We consider three types of ATL monomers, depending on their nucleotide bound state: GTP-bound monomers, T; GDP-bound monomers, D; and unbound ATL, A. The states TT and YY correspond to GTP-bound dimers and transition state dimers, respectively. Dimers at different nucleotide states are not considered. Transition state dimers, YY, are considered to be stable, and therefore require P_i release to dissociate. For simplicity's sake, we assume that hydrolysis and P_i release proceed at rates k_{hyd} and k_{rel}, respectively, and occur simultaneously in both monomers of a dimer.

The surface concentrations of the various ATL states are then given by the following kinetic equations, where we designate the ATL populations of the two vesicles by subscripts (α) and (β), and populations common to both vesicles by $(\alpha\beta)$:

$$\frac{d\left[A_\alpha\right]}{dt} = -j_{on}^{(GTP)}\left[A_\alpha\right]C_{GTP} + j_{off}^{(GTP)}\left[T_\alpha\right] - j_{on}^{(GDP)}\left[A_\alpha\right]C_{GDP} + j_{off}^{(GDP)}\left[D_\alpha\right] \qquad \textbf{(3.1)}$$

$$\frac{d\left[T_\alpha\right]}{dt} = j_{on}^{(GTP)}\left[A_\alpha\right]C_{GTP} - j_{off}^{(GTP)}\left[T_\alpha\right] + k_{off}^{(GTP)}\left(2\left[TT_\alpha\right] + \left[TT_{\alpha\beta}\right]\right) - k_{on}^{(GTP)}\left(2\left[T_\alpha\right]^2 + \chi\left[T_\alpha\right]\left[T_\beta\right]\right) \quad \textbf{(3.2)}$$

$$\frac{d\left[D_\alpha\right]}{dt} = k_{rel}\left(\left[YY_{\alpha\beta}\right] + 2\left[YY_\alpha\right]\right) + j_{on}^{(GDP)}\left[A_\alpha\right]C_{GDP} - j_{off}^{(GDP)}\left[D_\alpha\right] \quad \textbf{(3.3)}$$

$$\frac{d\left[TT_\alpha\right]}{dt} = k_{on}^{(GTP)}\left[T_\alpha\right]^2 - k_{off}^{(GTP)}\left[TT_\alpha\right] - k_{hyd}\left[TT_\alpha\right] \quad \textbf{(3.4)}$$

$$\frac{d\left[YY_\alpha\right]}{dt} = k_{hyd}\left[TT_\alpha\right] - k_{rel}\left[YY_\alpha\right] \quad \textbf{(3.5)}$$

$$\frac{d\left[A_\beta\right]}{dt} = -j_{on}^{(GTP)}\left[A_\beta\right]C_{GTP} + j_{off}^{(GTP)}\left[T_\beta\right] - j_{on}^{(GDP)}\left[A_\beta\right]C_{GDP} + j_{off}^{(GDP)}\left[D_\beta\right] \quad \textbf{(3.6)}$$

$$\frac{d\left[T_\beta\right]}{dt} = j_{on}^{(GTP)}\left[A_\beta\right]C_{GTP} - j_{off}^{(GTP)}\left[T_\beta\right] + k_{off}^{(GTP)}\left(2\left[TT_\beta\right] + \left[TT_{\alpha\beta}\right]\right) - k_{on}^{(GTP)}\left(2\left[T_\beta\right]^2 + \chi\left[T_\alpha\right]\left[T_\beta\right]\right) \quad \textbf{(3.7)}$$

$$\frac{d\left[D_\beta\right]}{dt} = k_{rel}\left(\left[YY_{\alpha\beta}\right] + 2\left[YY_\beta\right]\right) + j_{on}^{(GDP)}\left[A_\beta\right]C_{GDP} - j_{off}^{(GDP)}\left[D_\beta\right] \quad \textbf{(3.8)}$$

$$\frac{d\left[TT_\beta\right]}{dt} = k_{on}^{(GTP)}\left[T_\beta\right]^2 - k_{off}^{(GTP)}\left[TT_\beta\right] - k_{hyd}\left[TT_\beta\right] \quad \textbf{(3.9)}$$

$$\frac{d\left[YY_\beta\right]}{dt} = k_{hyd}\left[TT_\beta\right] - k_{rel}\left[YY_\beta\right] \quad \textbf{(3.10)}$$

$$\frac{d\left[TT_{\alpha\beta}\right]}{dt} = k_{on}^{(GTP)}\chi\left[T_\alpha\right]\left[T_\beta\right] - k_{off}^{(GTP)}\left[TT_{\alpha\beta}\right] - k_{hyd}\left[TT_{\alpha\beta}\right] \quad \textbf{(3.11)}$$

$$\frac{d\left[YY_{\alpha\beta}\right]}{dt} = k_{hyd}\left[TT_{\alpha\beta}\right] - k_{rel}\left[YY_{\alpha\beta}\right] \quad \textbf{(3.12)}$$

, where C_{GTP} is the concentration of GTP. The kinetic rates used for GTP and GDP binding and dissociation are (12): $j_{on}^{(GTP)} = 0.32 \quad \mu M^{-1}s^{-1}$, $j_{on}^{(GDP)} = 0.4 \quad \mu M^{-1}s^{-1}$, $j_{off}^{(GTP)} = 4 \quad s^{-1}$, $j_{off}^{(GDP)} = 4.8 \quad s^{-1}$.

The rate constants for dimer formation and dissociation for ATL proteins in bulk are $K_{on}^{(GTP)} = 0.32 \quad \mu M^{-1}s^{-1}$, $k_{off}^{(GTP)} = 0.16 \quad s^{-1}$, in the GTP-bound state (12). As the rate constant for dimerization of membrane-bound ATL, $k_{on}^{(GTP)}$ is unknown, we estimate

$$k_{on}^{(GTP)} = \frac{1}{L_{ATL}} K_{on}^{(GTP)} \qquad \textbf{(4)}$$

While the overall P_i release rate during steady-state GTP hydrolysis has been measured as $4.1 \mu M$ $P_i/\mu M$ ATL x min (12), the individual kinetic parameters for hydrolysis and P_i release are unknown. We therefore fit k_{rel} for a range of k_{hyd} values that correspond to the observed rate of P_i release:

$$k_{rel} = k_{rel}^{(fit)}\left(k_{hyd}\right) \qquad \textbf{(5)}$$

Tethering of vesicles

We solve the resulting set of differential equations numerically, to obtain the rate of formation of N trans dimers between two vesicles, $K_{trans}(N)$, for $N = 1,2\ldots$ For tethers to form, vesicles must first diffuse into the distance range for trans dimer formation, δ, at a rate $K_{diffuse} = 4\pi\delta D_{ves}$. The diffusion constant for vesicles, D_{ves}, is approximated using the Stokes-Einstein relation,

$$D_{ves} = \frac{k_B T}{6\pi\eta R} \qquad \textbf{(6)}$$

, where $\eta = 9 \cdot 10^{-4} poise$. The overall tethering rate, K_{tether}, is given by

$$K_{tether} = \frac{K_{trans}(N) \cdot K_{diffuse}}{K_{trans}(N) + K_{diffuse}} \qquad \textbf{(7)}$$

For all parameter values, we find $K_{trans}(N) << K_{diffuse}$, giving $K_{tether} \approx K_{trans}(N)$. In other words, diffusion of the vesicles is not rate-limiting.

The resulting time-dependent tethering of vesicles is calculated numerically for a liposome concentration of $1.6 \cdot 10^{15}$ vesicles per liter, 200 ATL monomers per vesicle, and $C_{GTP} = 2mM$. This vesicle concentration corresponds to ~0.6 mM lipids, assuming that the thickness of the lipid bilayer is 5 nm, and the average surface area of each phospholipid is 70 Å^2 (13). The number of ATL monomers per vesicle corresponds to ~1:1,000 protein:lipid ratio. The half-life time for vesicle tethering was calculated for a range of k_{hyd} and N values, as shown in Fig. S11. Vesicle tethering as a function of time is shown for a representative scenario with $k_{hyd} = 0.76\ s^{-1}$, $k_{rel} = 0.08\ s^{-1}$ in Fig. 9.

The role of transition state ATL monomers

We investigated the possible effect of GTP hydrolysis and P_i release in monomeric ATL, with the rates $k_{hyd}^{(M)}$ and $k_{rel}^{(M)}$, respectively. These reactions are considered in addition to those of hydrolysis and P_i release in ATL dimers. In this scheme, we include a monomeric population of the transition state, Y, with the rate equations:

$$\frac{d\left[Y_\alpha\right]}{dt} = k_{hyd}^{(M)}\left[T_\alpha\right] - k_{rel}^{(M)}\left[Y_\alpha\right] - 2k_{on}^{(GDP-P)}\left[Y_\alpha\right]^2 + 2k_{off}^{(GDP-P)}\left[YY_\alpha\right] + k_{off}^{(GDP-P)}\left[YY_{\alpha\beta}\right] \quad \textbf{(3.13)}$$

$$\frac{d\left[Y_\beta\right]}{dt} = k_{hyd}^{(M)}\left[T_\beta\right] - k_{rel}^{(M)}\left[Y_\beta\right] - 2k_{on}^{(GDP-P)}\left[Y_\beta\right]^2 + 2k_{off}^{(GDP-P)}\left[YY_\beta\right] + k_{off}^{(GDP-P)}\left[YY_{\alpha\beta}\right] \quad \textbf{(3.14)}$$

, and introduce the following corrections to the rate equations given above:

$$\frac{d\left[T_\alpha\right]}{dt} = \ldots\ - k_{hyd}^{(M)}\left[T_\alpha\right] \quad \textbf{(3.2B)}$$

$$\frac{d\left[D_\alpha\right]}{dt} = \ldots\ + k_{rel}^{(M)}\left[Y_\alpha\right] \quad \textbf{(3.3B)}$$

$$\frac{d\left[T_\beta\right]}{dt} = \ldots\ - k_{hyd}^{(M)}\left[T_\beta\right] \quad \textbf{(3.7B)}$$

$$\frac{d\left[D_\beta\right]}{dt} = \ldots\ + k_{rel}^{(M)}\left[Y_\beta\right] \quad \textbf{(3.8B)}$$

$$\frac{d\left[YY_{\alpha}\right]}{dt} = \ldots \quad + k_{on}^{(GDP-P)}\left[Y_{\alpha}\right]^2 - k_{off}^{(GDP-P)}\left[YY_{\alpha}\right] \qquad \textbf{(3.5B)}$$

$$\frac{d\left[YY_{\beta}\right]}{dt} = \ldots \quad + k_{on}^{(GDP-P)}\left[Y_{\beta}\right]^2 - k_{off}^{(GDP-P)}\left[YY_{\beta}\right] \qquad \textbf{(3.10B)}$$

$$\frac{d\left[YY_{\alpha\beta}\right]}{dt} = \ldots \quad + k_{on}^{(GDP-P)}\chi\left[Y_{\alpha}\right]\left[Y_{\beta}\right] - k_{off}^{(GDP-P)}\left[YY_{\alpha\beta}\right] \qquad \textbf{(3.12B)}$$

We estimate the rate constants for dimerization of transition state monomers as $k_{on}^{(GDP-P)} = 0.006 \quad \mu M^{-1}s^{-1}/L_{ATL}$ (12), and take into account that there is no direct dissociation of transition state dimers, $k_{off}^{(GDP-P)} = 0 \ s^{-1}$ (see Fig. 7).

We find that vesicle tethering is qualitatively unaffected by this addition to the model, indicating that the dominant mode of stable trans dimer formation is via dimerization and subsequent hydrolysis of GTP-bound ATL.

In order to simulate the effect of GDP/AlF_4^- on vesicle tethering, we set

$$k_{hyd}^{(M)} = k_{hyd} = \infty \qquad \textbf{(8.1)}$$

$$k_{rel}^{(M)} = k_{rel} = 0 \qquad \textbf{(8.2)}$$

We find that under such conditions, tethering of vesicles by ATL is severely impaired. This is explained by the fact that transition state trans dimers cannot form by hydrolysis of GTP-bound trans dimers. While monomeric ATL containing bound GDP/AlF_4^- may still dimerize, the available pool of monomers on each vesicle is rapidly depleted due to the formation of stable transition state cis dimers. As a result, tethering of vesicles is only possible for a short time after addition of GDP/AlF_4^- and then plateaus. Simulated tethering in the presence of GDP/AlF_4^- for a range of *N* values is shown as dashed lines in Fig. 9.

SI Figures

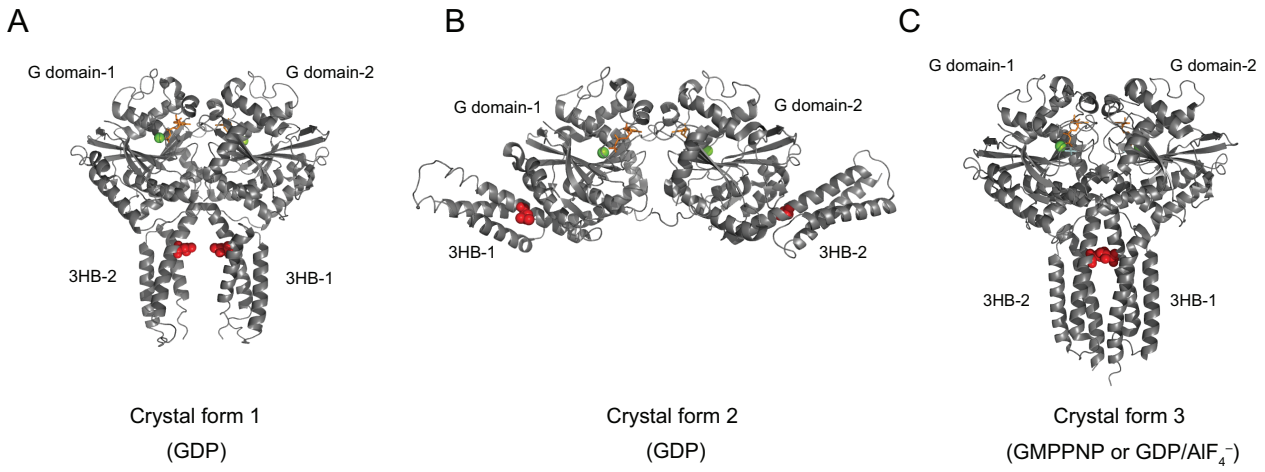

Fig. S1. Crystal structures of the cytosolic domain of human ATL1.

(A) Crystal form 1 of GDP-bound ATL1 (1, 11). The GTPase (G) domain and three-helix bundle (3HB) of each molecule in the dimer are indicated. The nucleotide is shown in stick representation in orange, and the magnesium ion is shown as a green sphere. Fluorescent probes for FRET were incorporated at position L357 (highlighted with red spheres) in the 3HB (corresponding to L332 in Drosophila ATL). PDB accession code: 3QNU.

(B) As in *(A),* but with crystal form 2 of GDP-bound ATL1 (1, 11). PDB accession code: 3QOF.

(C) As in *(A)*, but with crystal form 3 of ATL1, which contains either bound GDP/AlF_4^- or GMPPNP (12). Here, the molecules are bound to GDP/AlF_4^-, with the AlF_4^- shown in stick representation in light blue. PDB accession code: 4IDO.

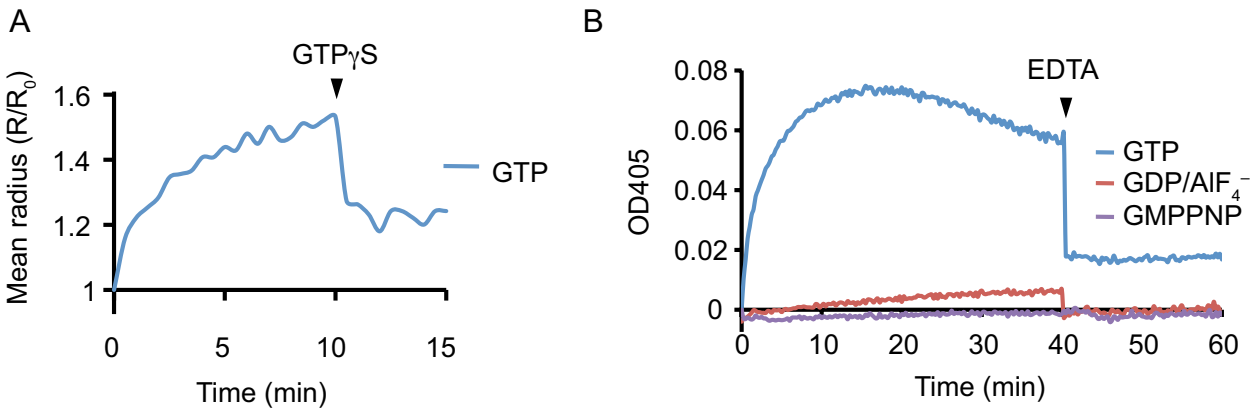

Fig. S2. ATL-mediated vesicle tethering and fusion requires GTP hydrolysis.
(A) The tethering and fusion of ATL-containing proteolipsomes (protein:lipid ratio 1:2,000) was followed after addition of 1 mM GTP by dynamic light scattering. The size of the vesicles was normalized to that determined at time zero (R/R_0). GTPγS (5 mM) was added after 10 min to out-compete GTP, and thereby terminate GTP hydrolysis by ATL.
(B) As in *(A)*, except proteoliposomes containing ATL at a protein:lipid ratio of 1:1,000 were used, and the size increase was followed by the absorbance at 405 nm after the addition of the indicated nucleotides. EDTA was added after 40 min to chelate Mg^{2+} and inactivate ATL.

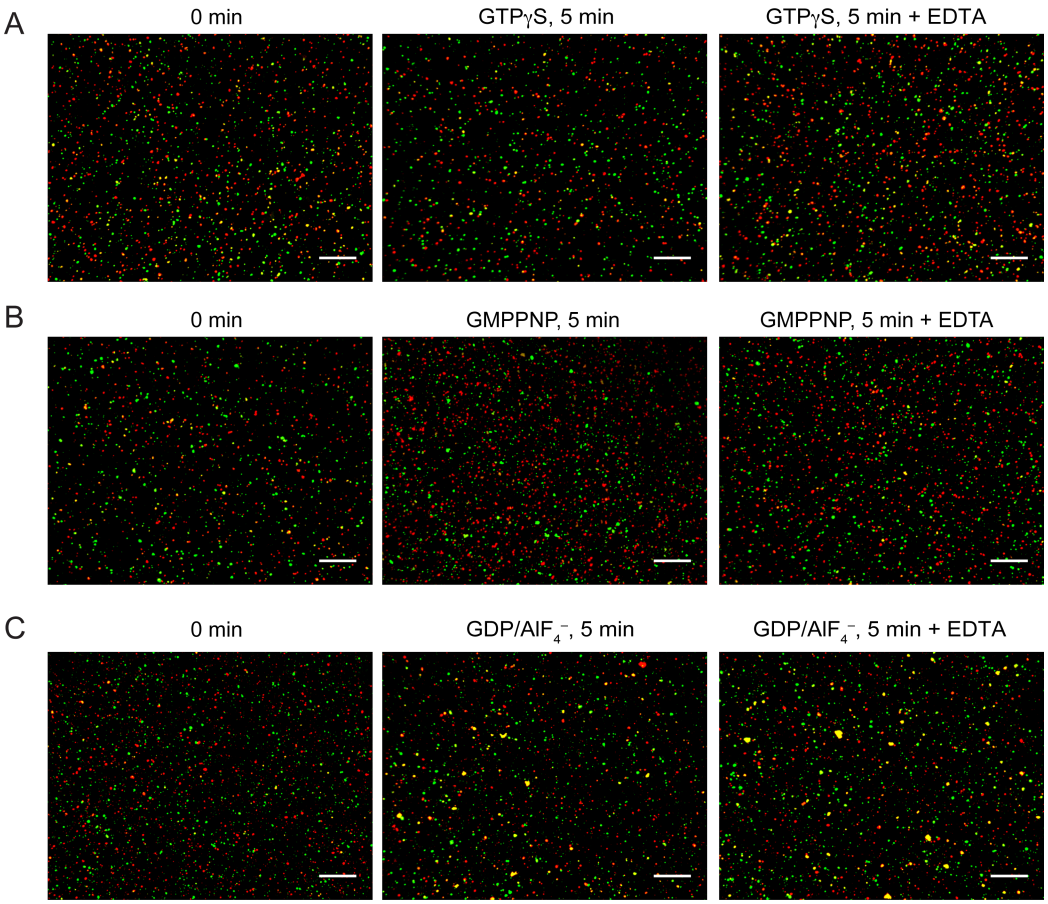

Fig. S3. ATL-mediated tethering and fusion followed by a visual assay.

(A) Wild type ATL-containing proteoliposomes (protein: lipid ratio 1:1,000), which also contained either Texas Red- or Oregon Green-labeled lipids, were mixed at a 1:1 ratio (total lipid concentration: 0.6 mM). One aliquot was analyzed immediately, a second was incubated at 37°C with 1 mM GTPγS for 5 min, and a third with GTPγS followed by incubation with 10 mM EDTA. All samples were diluted, spotted onto a coverslip, and visualized by confocal microscopy. Scale bar = 10 μm.

(B) As in *(A)*, but with 1 mM GMPPNP.

(C) As in *(A)*, but with GDP/AlF_4^-, generated by adding 1 mM GDP, 10 mM NaF, and 0.5 mM $AlCl_3$ to the reaction.

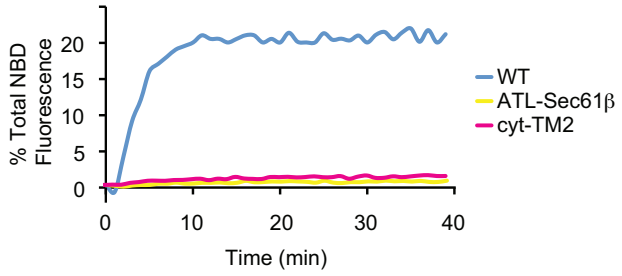

Fig. S4. ATL mutants with altered TM segments are fusion-defective.

Wild type (WT) ATL or ATL mutants with altered TM segments (ATL-Sec61β or cyt-TM2; see Fig. 3A) were reconstituted at a protein:lipid ratio of 1:2,000 into donor and acceptor vesicles. GTP-dependent lipid mixing was monitored by the de-quenching of a nitrobenzoxadiazole (NBD)-labeled lipid present in the donor vesicles. The data were normalized with respect to the fluorescence observed after addition of detergent.

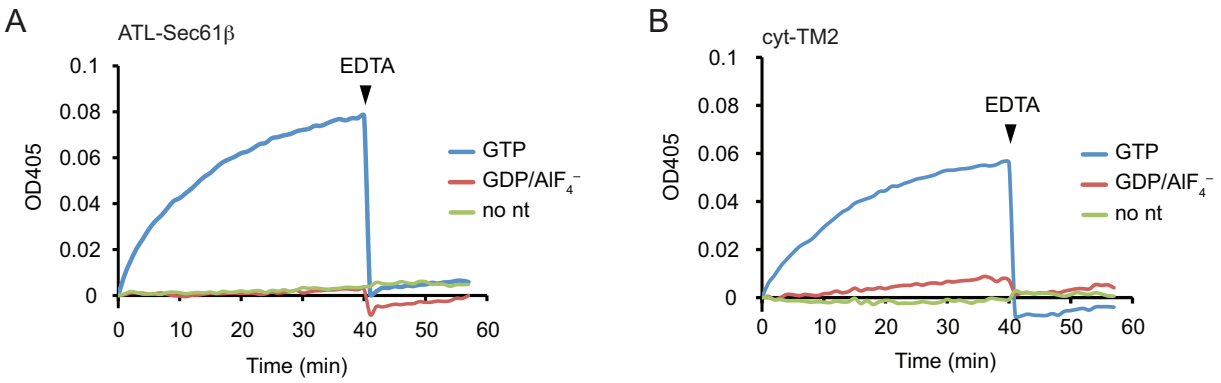

Fig. S5. Membrane tethering mediated by ATL-Sec61β or cyt-TM2 requires GTP hydrolysis.

(A) The tethering of vesicles containing ATL-Sec61*β* (protein:lipid ratio 1:1,000) was determined by the absorbance at 405 nm in the presence of GTP, GDP/AlF_4^-, or in the absence of nucleotide (no nt). EDTA was added after 40 min to chelate Mg^{2+} and inactivate ATL.

(B) As in *(A),* but with vesicles containing cyt-TM2 (protein:lipid ratio 1:1,000).

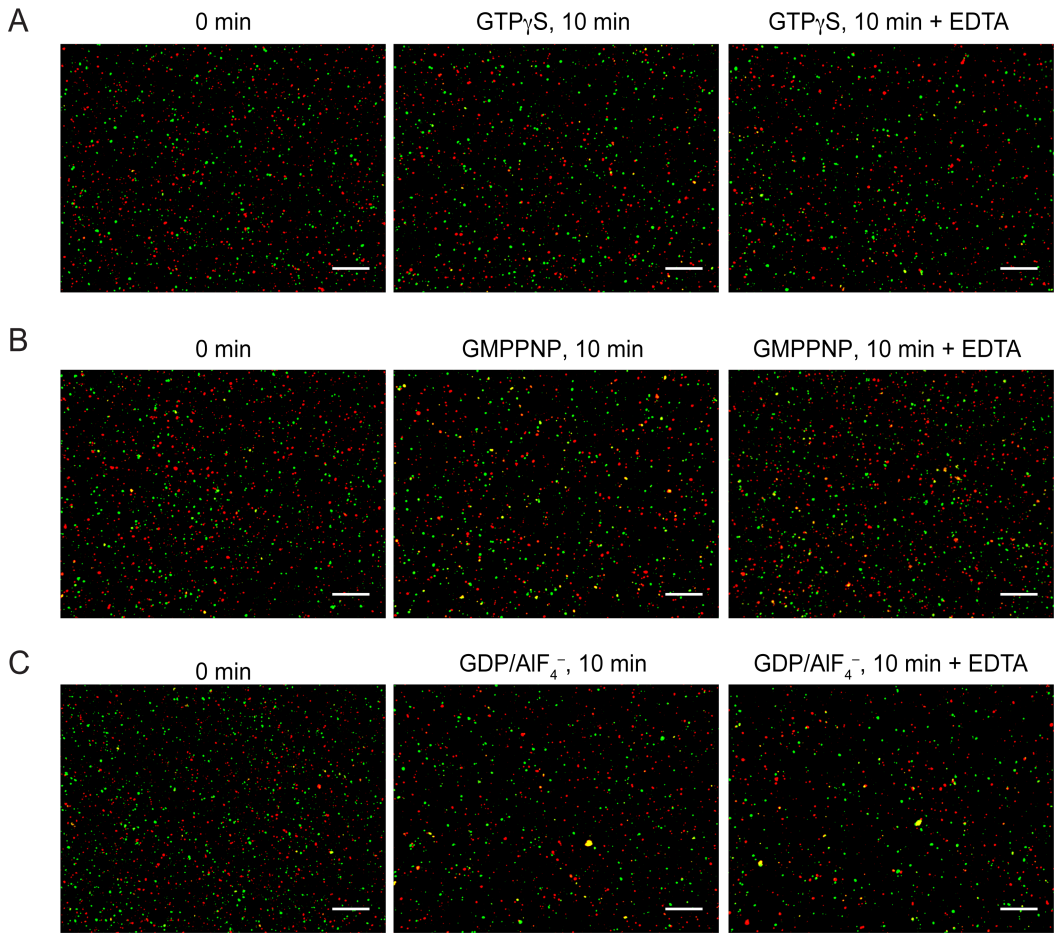

Fig. S6. Visual membrane tethering mediated by ATL-Sec61β requires GTP hydrolysis.

(A) Proteoliposomes containing ATL-Sec61β (protein:lipid ratio 1:1,000) and either Texas-Red or Oregon-Green labeled lipids were mixed at a 1:1 ratio (total lipid concentration: 0.6 mM). One aliquot was analyzed immediately, a second was taken after incubation at 37°C with 1 mM GTPγS for 10 min, and a third after incubation with GTPγS followed by addition of 10 mM EDTA. All samples were diluted, spotted onto a coverslip, and visualized by confocal microscopy. Scale bar = 10 μm.

(B) As in *(A)*, but with 1 mM GMPPNP.

(C) As in *(A)*, but with GDP/AlF_4^-, generated by adding 1 mM GDP, 10 mM NaF, and 0.5 mM $AlCl_3$.

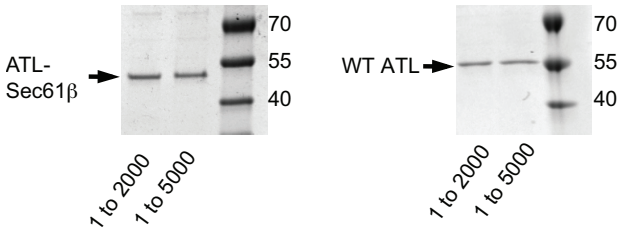

Fig. S7. Determination of the total ATL amounts in a tethering and fusion assay.

Samples of proteoliposomes (1.5 mM lipids) containing ATL-Sec61β or wild type (WT) ATL at protein:lipid ratios of 1:2,000 or 1:5,000. The total amounts of ATL (4 μl and 10 μl of 1:2,000 and 1:5,000 reconstitutions, respectively) used for experiments in Fig. 6A and 6B were subjected to SDS/PAGE and Coomassie Blue staining. The rightmost lane shows molecular weight markers, with sizes indicated in kilodaltons.

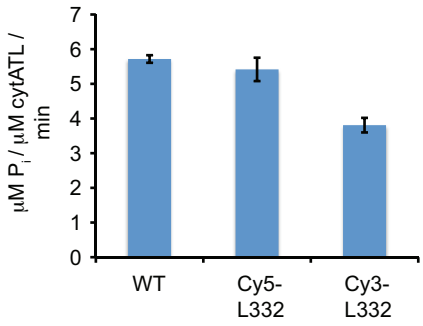

Fig. S8. Fluorescently labeled ATL proteins have similar GTPase activities as wild-type protein.

Drosophila cytATL with fluorescent probes at position 332 was generated in *E. coli* by suppression of an amber codon with azidophenylalanine-charged suppressor tRNA (4). The protein was then purified with a C-terminal His_6 tag and modified with Cy3 or Cy5 fluorescent dyes using Cu^{2+}-free click chemistry. The GTPase activities of the labeled proteins and of wild-type cytATL were determined by measuring the amount of P_i released. Shown are the means and standard errors of the means of three experiments.

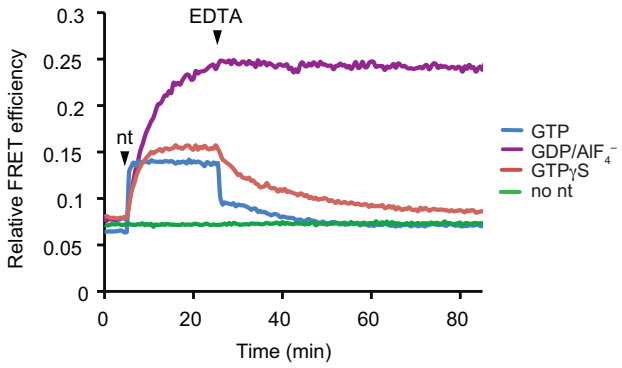

Fig. S9. Formation and dissociation of ATL dimers determined by FRET. *Drosophila* cytATL, containing an amber stop codon in the 3HB at position 332, was expressed in *E. coli* in the presence of azidophenylalanine-charged suppressor tRNA (4). The protein was purified and modified with Cy3 or Cy5 fluorescent dyes using Cu^{2+}-free click chemistry. The labeled proteins were mixed 1:1 and the indicated nucleotide (nt) or no nucleotide (no nt) was added at the time point indicated. FRET was determined by exciting the donor dye (Cy3) at 537 nm and measuring the emission of the donor and acceptor (Cy5) dyes at 570 nm and 667 nm, respectively. FRET is expressed as $I_A/(I_A+I_D)$, where I_A and I_D are fluorescence intensities of the acceptor and donor emission, respectively. EDTA (18 mM) was added to the reactions at the time point indicated.

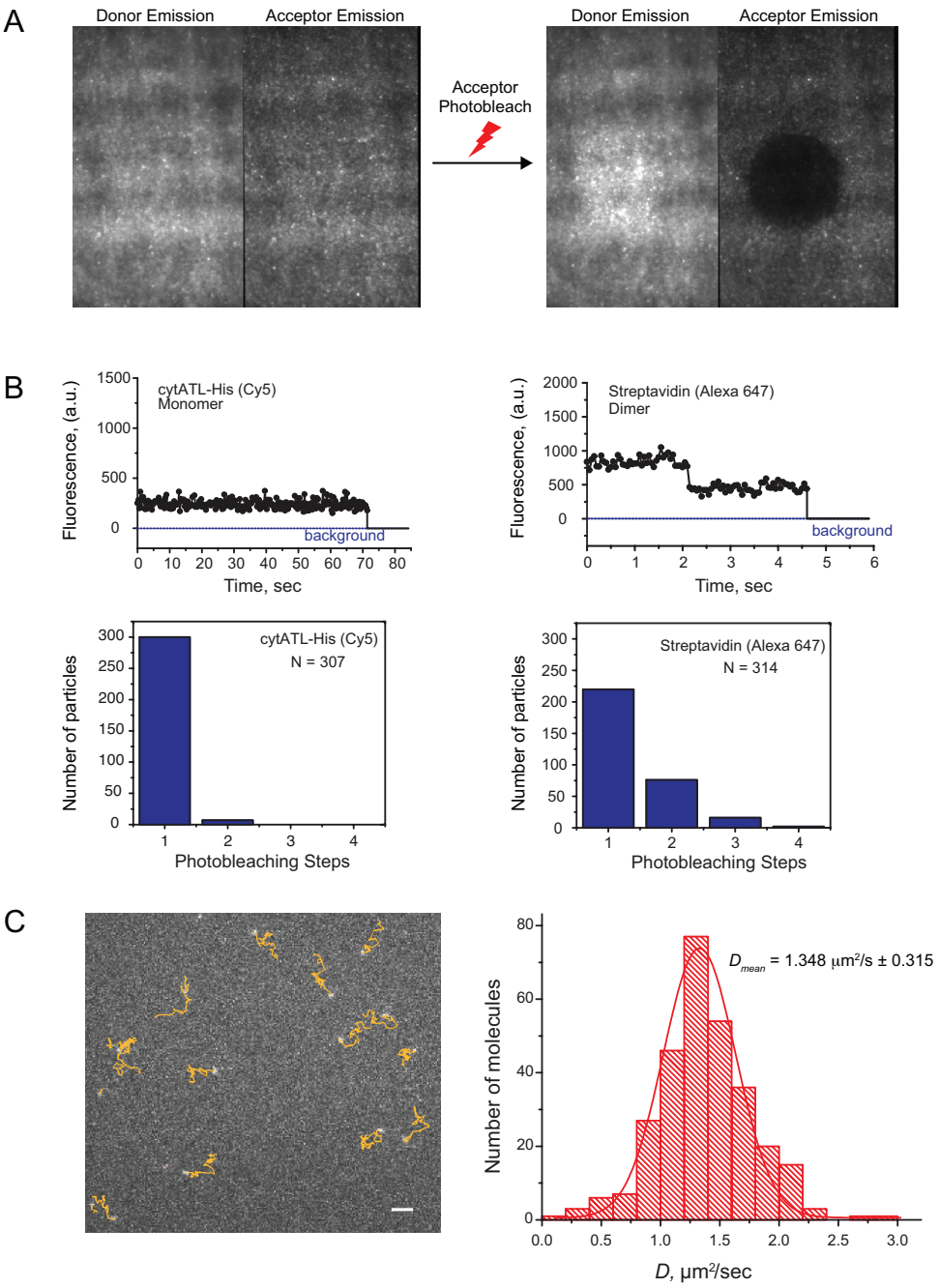

Fig. S10. Characterization of fluorescent ATL molecules on a supported bilayer. *(A)* Cy3- and Cy5-labeled cytATL-His were mixed (7 nM each) and added to a supported bilayer with Ni^{2+}-NTA lipids. GDP/AlF_4^- was subsequently added. The donor dye, Cy3, was excited with a laser line of 561 nm and both Cy3 (donor) and Cy5 (acceptor) fluorescence was visualized using a TIRF microscope (left panel). In the right panel, a circular area of Cy5-labeled cytATL-His was photobleached with the 647 nm laser line before imaging as before.

Fig. S10. Characterization of fluorescent ATL molecules on a supported bilayer (continued).

(B) Cy5-labeled cytATL-His (0.2 nM) was added to a supported bilayer with Ni^{2+}-NTA lipids in the presence of GDP/AlF_4^-. The dye was excited with a 647 nm laser, and imaged with a TIRF microscope. The fluorescence of individual molecules was tracked using particle tracking software (7) and monitored for spontaneous photobleaching. Shown is a photobleaching event for a single cytATL-His particle (left panel). The lower left panel shows a histogram of the distribution of bleaching steps per particle, with the number of particles analyzed (N). A control was performed with Alexa 647-labeled streptavidin added to a bilayer containing biotinylated lipids (right panels). The protein contains ~3 dyes per tetramer, explaining why multiple bleaching steps are observed per particle.

(C) Cy5-labeled cytATL-His was added to a bilayer and visualized by TIRF microscopy. The particles were tracked as in *(B).* An image showing the random walks (orange lines) taken by cytATL molecules is shown (left panel; scale bar = 3 μm). The apparent diffusion coefficient, *D,* was calculated for tracked particles using moment-scaling spectrum analysis (9, 10). A histogram of the values of *D* is shown for 300 particles analyzed (right panel). The mean value of *D* was calculated from a Gaussian fit of the data.

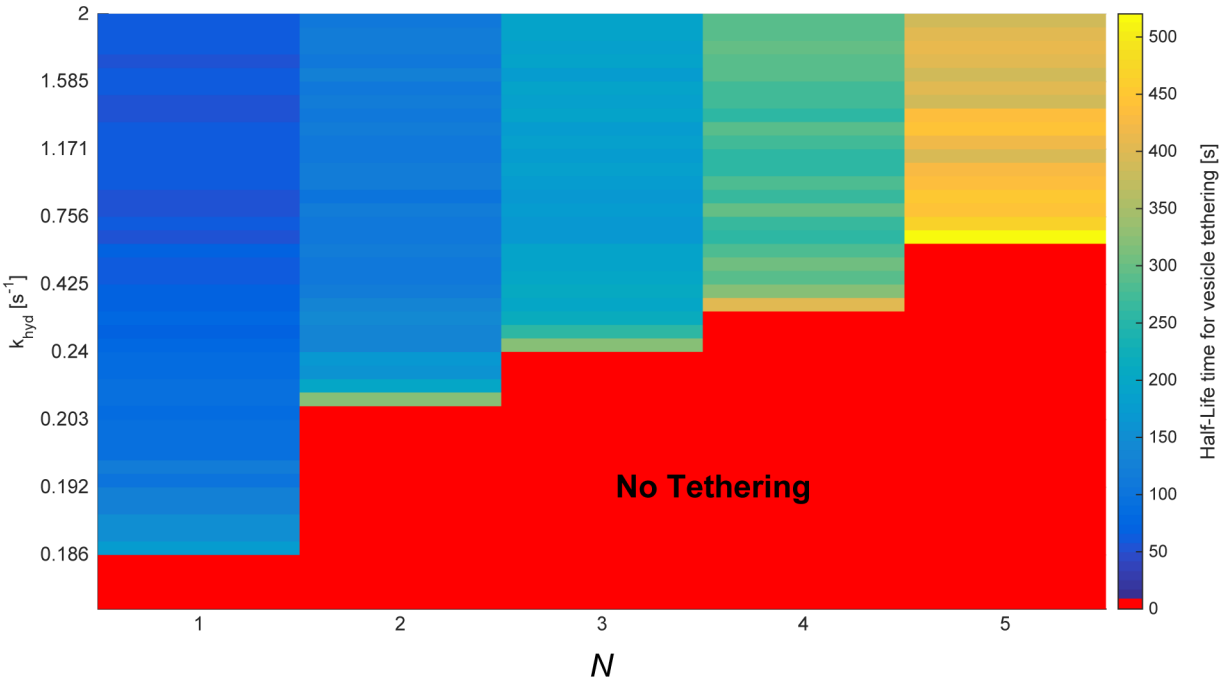

Fig. S11. Theoretical prediction of vesicle tethering.

The half-life time for binary vesicle tethering (i.e. the time it takes for 50% of the vesicles to become tethered) was calculated for a range of GTP hydrolysis rate constants, k_{hyd}, and of the minimal number (N) of trans dimers required for tethering. The P_i dissociation rate constant, k_{rel} was fitted to account for the previously measured P_i release rate of 4.1 μM P_i/μM ATL x min (12). The minimal hydrolysis rate required for tethering, k^*_{hyd}, ranges from , $k^*_{hyd} \simeq 0.19$ s^{-1} for $N = 1$ to $k^*_{hyd} \simeq 0.6$ s^{-1} for $N = 5$. The estimated half-life times are indicated by colors, with the scale given on the right. The figure shows that tethering is more pronounced with a lower number of trans dimers required for tethering, and with ATL spending more time in the transition state of GTP hydrolysis (when P_i release becomes rate-limiting).

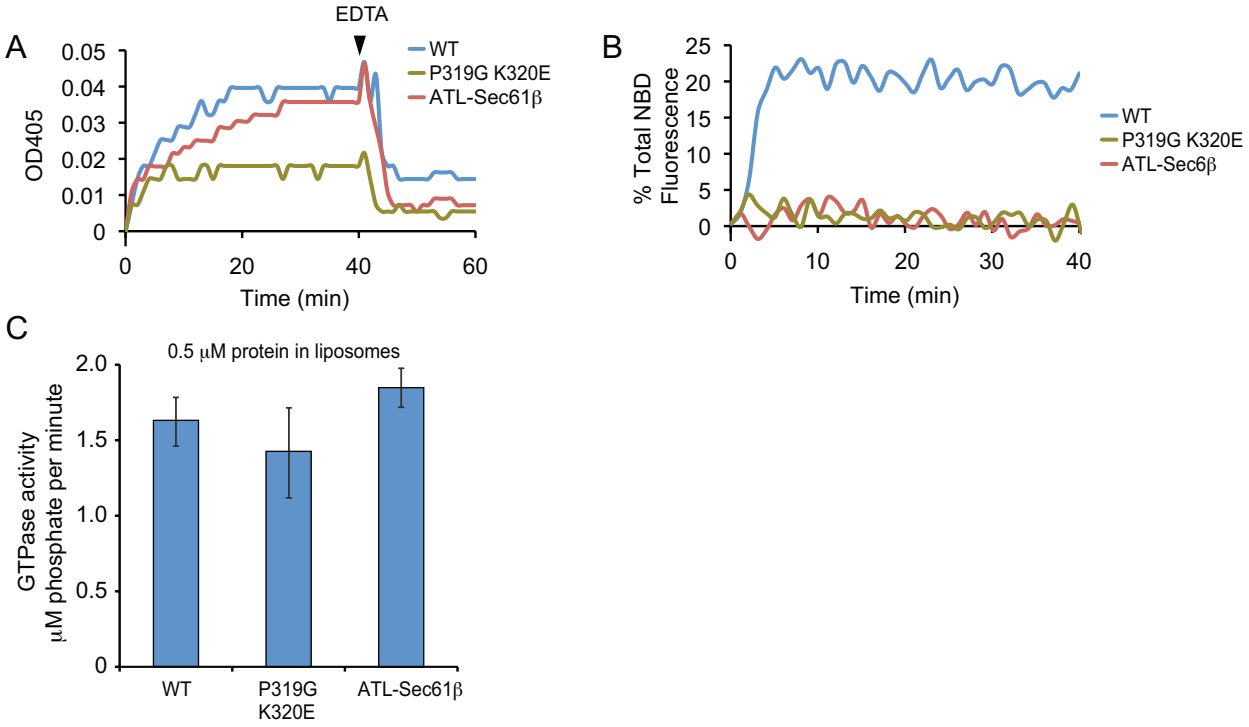

Fig. S12. Tethering, fusion, and GTPase activity of an ATL mutant carrying two point mutations in the linker between the G domain and 3HB.

(A) Proteoliposomes containing the P319G K320E ATL mutant (14), reported to be defective in generating the crossover configuration seen in crystal forms 1 and 3 (Fig. S1 and (1, 11, 12)), were tested for tethering and fusion by measuring the absorbance at 405 nm. Vesicles containing wild type (WT) or ATL-Sec61β were tested in parallel. In all cases the protein:lipid ratio was 1:2,000, and the reaction was started by the addition of GTP. At the time point indicated, EDTA was added to chelate Mg^{2+} and inactivate ATL.

(B) The indicated proteins were reconstituted at a protein:lipid ratio of 1:2,000 into donor and acceptor vesicles. GTP-dependent lipid mixing was monitored by the de-quenching of an NBD-labeled lipid present in the donor vesicles. The data were normalized with respect to the maximal fluorescence observed after addition of detergent.

(C) Proteoliposomes containing the indicated proteins were tested for GTPase activity by measuring the amount of P_i released. The means and standard errors of the means of three experiments are given.

SI References

1. Bian X, Klemm RW, Liu TY, Zhang M, Sun S*, et al.* (2011) Structures of the atlastin GTPase provide insight into homotypic fusion of endoplasmic reticulum membranes. *Proc Natl Acad Sci U S A* 108(10):3976-3981
2. Liu TY, Bian X, Sun S, Hu X, Klemm RW*, et al.* (2012) Lipid interaction of the C terminus and association of the transmembrane segments facilitate atlastin-mediated homotypic endoplasmic reticulum fusion. *Proc Natl Acad Sci U S A* 109(32):E2146-2154
3. Frey S & Gorlich D (2014) A new set of highly efficient, tag-cleaving proteases for purifying recombinant proteins. *J Chromatogr A* 1337:95-105
4. Young TS, Ahmad I, Yin JA, & Schultz PG (2010) An enhanced system for unnatural amino acid mutagenesis in E. coli. *J Mol Biol* 395(2):361-374
5. Orso G, Pendin D, Liu S, Tosetto J, Moss TJ*, et al.* (2009) Homotypic fusion of ER membranes requires the dynamin-like GTPase atlastin. *Nature* 460(7258):978-983
6. Schindelin J, Arganda-Carreras I, Frise E, Kaynig V, Longair M*, et al.* (2012) Fiji: an open-source platform for biological-image analysis. *Nat Methods* 9(7):676-682
7. Jaqaman K, Loerke D, Mettlen M, Kuwata H, Grinstein S*, et al.* (2008) Robust single-particle tracking in live-cell time-lapse sequences. *Nat Methods* 5(8):695-702
8. Aguet F, Antonescu CN, Mettlen M, Schmid SL, & Danuser G (2013) Advances in analysis of low signal-to-noise images link dynamin and AP2 to the functions of an endocytic checkpoint. *Dev Cell* 26(3):279-291
9. Ewers H, Smith AE, Sbalzarini IF, Lilie H, Koumoutsakos P*, et al.* (2005) Single-particle tracking of murine polyoma virus-like particles on live cells and artificial membranes. *Proc Natl Acad Sci U S A* 102(42):15110-15115
10. Ferrari R, Manfroi AJ, & Young WR (2001) Strongly and weakly self-similar diffusion. *Physica D: Nonlinear Phenomena* 154(1-2):111-137
11. Byrnes LJ & Sondermann H (2011) Structural basis for the nucleotide-dependent dimerization of the large G protein atlastin-1/SPG3A. *Proc Natl Acad Sci U S A* 108(6):2216-2221
12. Byrnes LJ, Singh A, Szeto K, Benvin NM, O'Donnell JP*, et al.* (2013) Structural basis for conformational switching and GTP loading of the large G protein atlastin. *Embo J* 32(3):369-384
13. Lewis BA & Engelman DM (1983) Lipid bilayer thickness varies linearly with acyl chain length in fluid phosphatidylcholine vesicles. *J Mol Biol* 166(2):211-217
14. Saini SG, Liu C, Zhang P, & Lee TH (2014) Membrane tethering by the atlastin GTPase depends on GTP hydrolysis but not on forming the cross-over configuration. *Mol Biol Cell* 25(24):3942-3953